Tellus SERIES B CHEMICAL AND PHYSICAL METEOROLOGY
PUBLISHED BY THE INTERNATIONAL METEOROLOGICAL INSTITUTE IN STOCKHOLM

Tellus (2010), 62B, 109–116
Printed in Singapore. All rights reserved

TELLUS

Monitoring of urban air pollution from MODIS aerosol data: effect of meteorological parameters

By YONG ZHA[1]*, JAY GAO[2], JIANJUN JIANG[1], HENG LU[1] and JIAZHU HUANG[1], [1]*Key Laboratory of Virtual Geographic Environment, Ministry of Education, College of Geographic Science, Nanjing Normal University, Nanjing 210097, China*; [2]*School of Geography, Geology and Environmental Science, University of Auckland, Private Bag 92019, Auckland, New Zealand*

(Manuscript received 9 July 2009; in final form 13 January 2010)

ABSTRACT

Remote sensors designed specifically for studying the atmosphere have been widely used to derive timely information on air pollution at various scales. Whether the satellite-generated aerosol optical thickness (AOT) data can be used to monitor air pollution, however, is subject to the effect of a number of meteorological parameters. This study analyses the influence of four meteorological parameters (air pressure, air temperature, relative humidity, and wind velocity) on estimating particulate matter (PM) from MODIS AOT data for the city of Nanjing, China during 2004–2006. After the PM data were correlated with the AOT data that had been divided into four chronological seasons, a minimum correlation coefficient of 0.47 was found for the winter season, but a much stronger correlation ($r > 0.80$) existed in summer and autumn. Similar analyses were carried out after all observations were clustered into four groups based on their meteorological similarity using the K-Means analysis. Grouping caused more observations to be useable in the monitoring of air pollution than season-based analysis. Of the four groups, three had a correlation coefficient higher than 0.60. Grouping-based analysis enables the pollution level to be determined more accurately from MODIS AOT data at a higher temperature and relative humidity, but a lower air pressure and wind velocity. The accuracy of monitoring air pollution is inversely related to the pollution level. Thus, remote sensing monitoring of air pollution has its limits.

1. Introduction

Air pollution is a global issue that has caused massive economic loss. It is particularly serious in developing countries such as China where air quality has deteriorated considerably since 1978 when the nation embarked on an ambitious economic reform and revitalization program. Rapid industrialization and development of the automobile industry, in conjunction with construction, have contributed to the huge rise in suspended particulates in the air. Air pollution has exerted a grave consequence over the environment, people's lives and health, and even threatens the sustainability of social and economic development (Wang and Zha, 2006).

Air quality is usually monitored at fixed ground stations. Although ground measurements are able to indicate the concentration level of air pollutants and their temporal variations precisely, this method of monitoring is limited by its huge expense and sparse spatial coverage. The limited number of stations on the ground cannot depict the spatial pattern of pollutant concentration at a broad scale. Moreover, the observation made at the surface or near surface cannot capture the vertical variation of pollutants above it. By comparison, remote sensing is much more advantageous. It is able to yield timely information on air pollution over an extensive area quickly and inexpensively. It is becoming an acceptable alternative to ground observation thanks to the launch of sensors designed specifically to study aerosols. This method complements the ground-based observation (Mao et al., 2002). The aerosol product derived from satellite data not only provides a means of studying global and regional climate, but also enables the study of air pollution in urban areas from space. Owing to the improved capabilities of earth observation satellites, space-borne imagery has found increasing applications in monitoring urban air quality in conjunction with ground-based data (Engel-Cox et al., 2004a).

Of the various satellite data available, the MODerate resolution Imaging Spectroradiometer (MODIS) imagery has the finest temporal resolution of 12 h. Such a trait is highly desirable in studying the atmospheric composition in general, and aerosols in particular. MODIS imagery is capable of monitoring air

*Corresponding author.
e-mail: yzha@njnu.edu.cn
DOI: 10.1111/j.1600-0889.2010.00451.x

pollution at a scale ranging from local to regional to global (Chu et al., 2003; Engel-Cox et al., 2004b; Gupta et al., 2006). If jointly used with ground observations, MODIS aerosol optical thickness (AOT) data could be useful in accurately monitoring pollutants for the entire state of Texas (Hutchison, 2003; Hutchison et al., 2004, 2005). The principle behind remotely sensing air quality from space is underpinned by a relationship between reflectance recorded on satellite data and ground observed air pollution level. Li et al. (2004) reported a high degree of correlation between ground observed particulate concentrations and MODIS-derived AOT in Hong Kong. Moreover, there exists a high level of correlation between air pollution index (API) released by many Chinese municipal environmental monitoring stations and AOT (Liu et al., 2003). The existence of such correlation raises the feasibility of studying air pollution in urban areas from the AOT products of MODIS data that have a spatial resolution of 10 km. This feasibility has been corroborated by Li et al. (2003a) after comparing the MODIS AOT products with the corresponding data obtained in 2001 with a sunphotometer for the Beijing region. Wang and Christopher (2003) achieved a correlation coefficient of 0.7 between satellite-derived AOT and fine particulate matter (PM) measured at the surface at seven locations in Jefferson county, Alabama. Similar findings have been obtained in a number of cities in the Yangtze River delta (Liu et al., 2003). Therefore, the MODIS-derived AOT product provides a new means for studying air pollution. There is a unique correspondence between PM and API in Chinese cities on days when the air pollutants are dominated by PM10 rather than gaseous pollutants such as CO, SO_2 and NO_2. For instance, API = 50 when PM10 = 50 μgm^{-3}, API = 100 when PM10 = 150 μgm^{-3}, API = 200 when PM10 = 350 μgm^{-3}, API = 300 when PM10 = 420 μgm^{-3} and so on. Thus, it is possible to convert these two parameters interchangeably based on this relationship between API and PM10. At the same time, API can be reflected by AOT as API corresponds to a certain PM concentration level.

Nevertheless, it must be emphasized that PM or API is by no means synonymous to AOT. On the contrary, each has its own unique physical meaning. PM or API is determined by the mass of particulates. It refers mainly to the concentration of solid pollutants generated near the Earth's surface from vehicle exhaust and chimney discharge. It does not encompass such gaseous pollutants as CO, SO_2 and NO_2. This concentration level is subject strongly to air turbulence caused by atmospheric instability and vertical layer mixing. AOT refers to the cumulative vertical extinction coefficient of the solar radiation that is determined by the total amount of aerosols over the air column and their diameter. Thus, it exhibits a distinct spatiotemporal pattern of variation. For instance, in the Sichuan Basin of western China the mean AOT is maximal in spring due to the influence of dust storms (Li et al., 2003b). The western portion of the Basin maintained a high value year round, but the eastern part has a large seasonality of AOT.

It is impossible for AOT to reflect PM or API reliably under all meteorological circumstances even if the pollutants are overwhelmed by particulate matter. AOT and PM/API are closely correlated with each other only under certain kind of weather conditions. This close correlation enables the monitoring of PM/API from the AOT product of MODIS data statistically. In studying the correlation between AOT and PM/API, the seasonal variation is usually examined by partitioning all available observations into four chronological seasons, and then the correlation between the two variables is examined separately in each season (Wang, 2006). However, this treatment cannot reveal the meteorological conditions under which PM/API is monitored from AOT most reliably as the seasonality is related largely to temperature but not other meteorological parameters. This limitation can be overcome by grouping observations statistically in terms of meteorological similarity. This will considerably enhance our understanding of the influence of meteorological parameters on the monitoring of air quality by means of remote sensing that is very important in avoiding erroneous estimates.

The objective of this study is to explore the effect of meteorological parameters on monitoring air pollution as recorded in ground surveillance stations from MODIS-derived AOT data for the city of Nanjing, eastern China. The specific aims are: (1) to examine the influence of temperature (T), pressure (P), relative humidity (RH) and wind velocity (WV), all of which are considered as the common meteorological variables affecting AOT or PM (Zakey et al., 2004; Suresh and Desa, 2005; Lee and Kim, 2007), on the correlation between PM and AOT based on seasonal and clustered data in order to reveal the meteorological conditions at which the two are most closely correlated and (2) to compare the capability of grouping data by season and by meteorological similarity in monitoring air pollution from remote sensing-derived aerosol data.

2. Data and Analysis

2.1. PM and meteorological data

There is a high concentration of relatively large suspended particles in the atmosphere as a result of rapid industrialization and urbanization in developing China. Therefore, the Chinese Ministry of Environmental Protection makes use of PM_{10} (particulate matter with a diameter ≤ 10 μm) instead of the $PM_{2.5}$ as the indicator of daily air quality. Researchers have established that PM_{10} behaves just like $PM_{2.5}$ in terms of correlation with AOT derived from MODIS data (Engel-Cox et al., 2004b), even though such derived AOT may manifest chiefly $PM_{2.5}$ potentially. API are released by the Chinese Ministry of Environmental Protection to the public after the in situ measured PM_{10} data have been linearly converted to API. API is a parameter indicative of atmospheric pollution level. In China API is defined as 50 when $PM_{10} = 50$ μgm^{-3} or 100 if $PM_{10} = 150$ μgm^{-3}; API is defined as 200 at 350 μgm^{-3} of PM_{10} or 300 at 420 μgm^{-3} of PM_{10}.

Therefore, API = (PM_{10}–50) × (100 − 50)/(150 − 50) + 50 between 50 and 150 μgm^{-3} of PM_{10}, or API = (PM_{10}–150) × (200−100)/(350−150) + 100 when PM_{10} lies between 150 μgm^{-3} and 350 μgm^{-3}, or API = (PM_{10}–350) × (300 − 200)/(420−350) + 200 at the PM_{10} range of 350–420 μgm^{-3}. With the assistance of these equations it is possible to retrieve PM_{10} for every known API value.

Because the large majority of pollutants in most Chinese cities is predominantly particulates (Li et al., 2003a), it is possible to monitor air quality from the satellite data-derived AOT. The daily PM_{10} data used in this study were derived from daily API data, acquired from the Chinese Ministry of Environmental Protection. They were averaged from six observation stations distributed widely across the metropolitan area (976 km^2) of Nanjing. The meteorological data were collected from the Nanjing Meteorological Observation Station located at (118.8°E, 32.0°N) and 7.1 m a.s.l.

Nanjing City has a population of 5.37 million and an urban area of 976 km^2. This city is a comprehensive industrial base in the economically developed eastern China. Its location in the Yangtze River valley means that air pollutants are not so easily dispersed. Over the last few decades it has suffered from severe air pollution due to rapid economic development that has brought an abrupt rise in vehicles and widespread construction sites. Consequently, air quality has deteriorated drastically with frequent occurrence of hazy days, especially in winter.

2.2. MODIS AOT data

MODIS is a sensor aboard the Terra/Aqua Earth Observation System satellites. Its 36 spectral wavebands span over the visible light, near infrared and infrared portion of the spectrum with the finest spatial resolution being 250 m at a swath width of 2330 km. Such image properties make MODIS data the ideal candidate in remotely sensing terrestrial aerosol (King et al., 1992). The MODIS aerosol products are derived from channels 1 and 3 (visible light) with the assistance of band 7 (near infrared) using the dark pixel algorithm at a spatial resolution of 10 km. In this band the radiometric properties of dark objects are correlated closely to their ground reflectance in bands 1 and 3 (Kaufman et al., 1997a, b). Thus, the ground reflectance in bands 1 and 3 becomes known. The derived MODIS AOT is rendered as grey levels with a value from 0 to 3000 (unit: 10^{-3}). The AOT data analysed in this study span a period from 2004 to 2006. They are the averaged values of pixels across the entire metropolitan area (976 km^2) of Nanjing City.

2.3. Data analysis

All the collected data were screened first to remove those records observed on rainy and cloudy days. In the end, only 157 observations during the three-year period were retained for analysis. They were grouped into four chronological seasons of spring (March–May), summer (June–August), autumn (September–November) and winter (December–February). The four meteorological parameters in each season were statistically analysed. In addition, PM_{10} was correlated with AOT separately by season. The same analysis was subsequently performed on the observations that had been clustered into four groups using the K-Means clustering method. The maximum, minimum, mean, range and standard deviation of each meteorological parameter in each group were calculated, together with the PM_{10} data. Their properties were compared to their counterparts in the season-based results.

3. Results

3.1. Seasonal correlation of PM and AOT

Partitioning of the 157 observations into the four seasons results in the largest number of observations in spring ($n = 62$), but only 24 observations in summer. The scatterplots (Fig. 1) reveal that there exists a linear relationship between PM_{10} and AOT in all four seasons. Nevertheless, the accuracy of monitoring PM_{10} from AOT varies with seasonality. The regressional relationship is the strongest in summer (Fig. 1b), but the weakest in winter (Fig. 1d). Therefore, PM_{10} can be rather reliably estimated from AOT in summer and autumn (e.g. $R^2 > 0.6$), but much less so in spring and winter (e.g. $R^2 < 0.3$).

It is necessary to examine the meteorological conditions in different seasons in order to identify any patterns that are responsible for the observed seasonal variations in the R^2 value. As shown in Table 1, PM_{10} has a similarly low correlation coefficient of around 0.5 with AOT in both spring and winter, but a noticeably higher coefficient of around 0.83 in summer and autumn. Examination of figures in Table 1 does not bring out any obvious meteorological pattern for the close correlation in summer and autumn. For instance, air pressure is the highest and second highest in winter and autumn, respectively. However, temperature is similarly high in the mid-10 °C in both spring and autumn. Relative humidity is the highest in autumn, but very close to each other in spring and winter. By comparison, autumn has the calmest weather while summer is the windiest. Such a variation indicates that rarely a single meteorological variable is solely responsible for the correlation. Instead, it is the joint effects of a number of variables that make PM_{10} estimated from AOT.

In sum, it is impossible to ascertain the exact meteorological conditions that are responsible for the high correlation in the summer and autumn seasons, and the low correlation in winter and spring. The absence of any identifiable meteorological pattern accountable for the high/low correlation coefficient in Table 1 is due largely to the chronological partitioning of the data, which results in occurrence of the same value in multiple seasons. There are no clear-cut boundaries across different seasons. This problem can be overcome with clustering analysis.

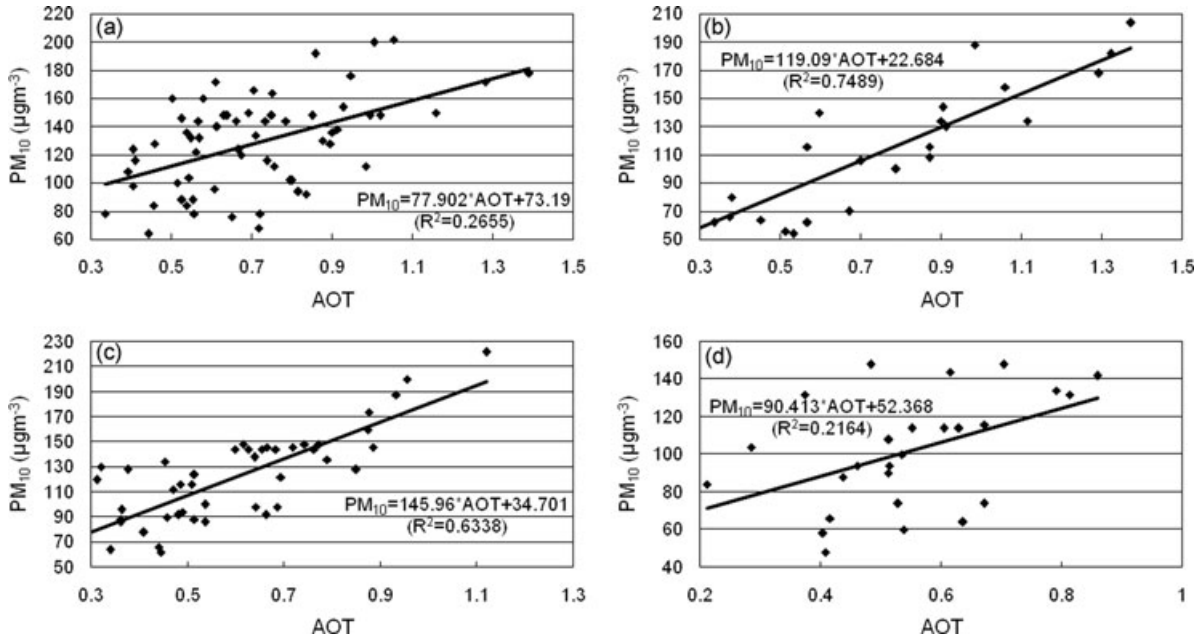

Fig. 1. Correlation between PM_{10} and MODIS-derived AOT value by season: (a) spring; (b) summer; (c) autumn and (d) winter.

Table 1. Seasonal correlation coefficient between PM_{10} and AOT and the statistical properties of the four meteorological parameters by season

Season (coefficient)	Statistical parameters	*P* (hPa)	*T* (°C)	RH (%)	WV (m s^{-1})
Spring (0.52)	Min	997.5	3.4	34	0.5
	Max	1031.6	25.7	80	4
	Rang	34.1	22.3	46	3.5
	Ave	1015.47	16.27	53.24	2.23
	SD	7.41	6.18	9.78	0.77
Summer (0.87)	Min	996.4	22.2	40	1
	Max	1014.2	32.3	73	4.3
	Rang	17.8	10.1	33	3.3
	Ave	1004.81	29.49	59.17	2.55
	SD	3.74	2.36	9.09	1.04
Autumn (0.80)	Min	1008.90	4.50	51.00	0
	Max	1029.90	28.20	81.00	4.30
	Rang	21.00	23.70	30.00	4.30
	Ave	1020.24	16.76	67.49	1.43
	SD	4.58	5.23	6.84	0.76
Winter (0.47)	Min	1017.7	−3	21	0.5
	Max	1036.5	12.8	70	4.7
	Rang	18.8	15.8	49	4.2
	Ave	1027.15	3.03	52.31	2.07
	SD	5.46	4.01	14.53	1.07

3.2. Correlation based on clustered data

In order to reveal the contribution of individual meteorological variables to the observed correlation between AOT and PM_{10}, it was decided that the entire dataset of 157 observations should be grouped into four categories, the same number as the four seasons in order to identify the impact of individual parameters on the correlation. This grouping was based on the K-Means clustering analysis in which the number of iterations was specified as 20. This clustering analysis was repeated five times, each time for one of the four meteorological criteria singularly and one time for all four parameters.

Table 2. Statistical properties of the four meteorological parameters after clustering analysis based on a single parameter

Group	Statistical parameters	P (hPa)	T (°C)	RH (%)	WV (m s^{-1})
1	Min	996.4	−3.0	21	0.0
	Max	1009.0	7.7	47	1.3
	Rang	12.6	10.7	26	1.3
	Ave	1004.87	3.06	39.00	0.97
	SD	2.88	2.99	7.00	0.32
2	Min	1010.0	8.4	48	1.4
	Max	1017.3	16.2	59	2.0
	Rang	7.3	7.8	11	0.6
	Ave	1013.79	12.61	53.58	1.76
	SD	2.17	2.15	3.11	0.18
3	Min	1017.5	16.5	60	2.1
	Max	1024.8	24.0	68	2.9
	Rang	7.3	7.5	8	0.8
	Ave	1020.95	20.57	64.15	2.44
	SD	2.12	2.22	2.36	0.26
4	Min	1025.0	24.9	69	3.0
	Max	1036.5	32.3	81	4.7
	Rang	11.5	7.4	12	1.7
	Ave	1029.33	29.14	73.10	3.63
	SD	3.13	2.26	3.53	0.53

Table 3. Correlation coefficients between PM_{10} and AOT after clustering analysis based on a single meteorological parameter

Grouping variable	Group 1	Group 2	Group 3	Group 4
P (hPa)	0.83	0.44	0.74	0.55
T (°C)	0.42	0.64	0.67	0.85
RH (%)	0.55	0.63	0.70	0.80
WV (m s^{-1})	0.80	0.48	0.72	0.72

After grouping, all the meteorological variables have a unique value range of their own (Table 2), in drastic contrast to those in Table 1. Their values change gradually from the first group to the last group. Correlation analysis indicates that grouping of all observations into four categories is conducive to improving the correlation between PM_{10} and AOT (Table 3). Apart from relative humidity and wind velocity, temperature and pressure each has only one group with a correlation coefficient smaller than its minimum counterpart in Table 1 (e.g. <0.47). The coefficients in other three groups have become very high (>0.55). Only temperature and relative humidity produce a correlation coefficient that varies regularly from group 1 to group 4. And the surface temperatures are very cold in group 1, compared to the other groups. Furthermore, the maximum coefficient occurs in the first group for pressure and wind velocity, but the last group for temperature and relative humidity.

The above analysis demonstrates that it is increasingly reliable to monitor PM_{10} from remote sensing-derived AOT when temperature and relative humidity are high, but pressure and wind velocity are low. Conversely, a low temperature and humidity combined with a high pressure and wind velocity weaken the correlation. Such meteorological conditions are able to account for the change in correlation completely because AOT is produced locally and the locally produced particulates are not dispersed laterally. Thus, the sensed pollution conditions are a realistic depiction of the reality on the ground.

To explore the joint effect of the four meteorological parameters, the same dataset was clustered into four groups using all four parameters simultaneously. Although the correlation coefficient stands at only 0.45 for one of the groups after grouping, the correlation coefficient is larger than 0.6 for the other three groups (Table 4). The correlation tends to be stronger when the atmospheric pressure is lower with the exception of group 3. Similarly, the coefficient is higher when the temperature and relative humidity are higher. The correlation becomes stronger at a lower wind velocity. Thus, if all four parameters are considered, the same conclusion holds true: a high correlation is associated with a high temperature and relative humidity, but a low pressure and wind velocity.

The above findings are physically explicable. Apparently, these two parameters are correlated closely to each other when AOT results chiefly from PM10 locally. In order to make the AOT value reflective primarily of local PM10, the surface layer must not have noticeable horizontal movements while vertical mixing is relatively strong. Such an atmospheric state occurs at a high temperature and relative humidity, but a low pressure

Table 4. Correlation coefficients between PM_{10} and AOT after clustering analysis based on all four meteorological parameters simultaneously and the statistical properties of the four meteorological parameters

Group (coefficient)	Statistical parameters	*P* (hPa)	*T* (°C)	RH (%)	WV (m s^{-1})
1 (0.45)	Min	1016.0	−3.0	21	1.3
	Max	1036.5	12.5	56	4.7
	Rang	20.5	15.5	35	3.4
	Ave	1027.45	5.24	41.35	2.40
	SD	5.23	4.68	9.06	0.86
2 (0.62)	Min	996.4	10.5	40	1.0
	Max	1020.3	32.3	62	4.3
	Rang	23.9	21.8	22	3.3
	Ave	1010.64	21.30	52.35	2.43
	SD	5.95	5.58	5.18	0.87
3 (0.77)	Min	1017.3	−1.8	53	0.0
	Max	1034.2	21.4	79	4.3
	Rang	16.9	23.2	26	4.3
	Ave	1022.84	11.43	65.45	1.46
	SD	3.85	6.16	5.91	0.84
4 (0.73)	Min	1000.5	18.0	61	0.5
	Max	1017.6	31.9	81	4.3
	Rang	17.1	13.9	20	3.8
	Ave	1009.40	25.38	69.03	1.99
	SD	4.93	4.90	5.57	0.86

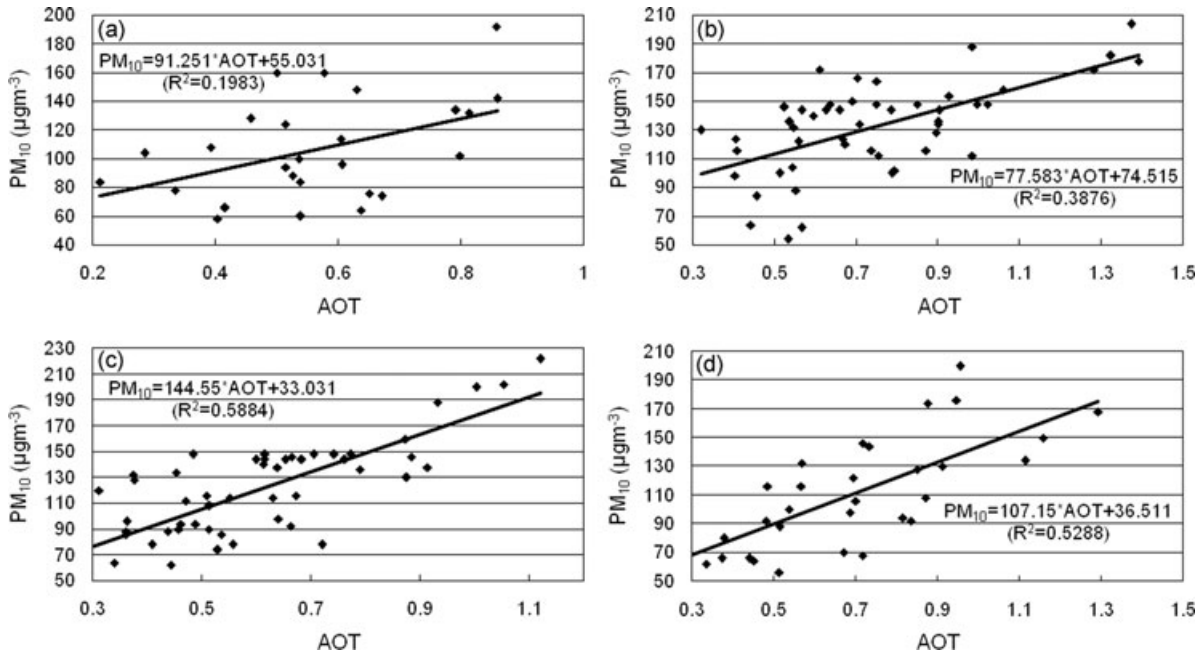

Fig. 2. The relationship between PM_{10} and AOT after all observations were grouped into four categories using the K-Means clustering analysis: (a) group 1; (b) group 2; (c) group 3 and (d) group 4.

and wind velocity. These conditions lead to the close correlation between AOT and PM10 mass.

As demonstrated in Fig. 2, group 1 has the lowest R^2 value. At 0.198, it is even lower than the smallest R^2 value for the season of winter. However, the R^2 value for the other three groups is relatively high. This means that grouping improves the correlation between PM_{10} and AOT. The most reliable model takes the following formula:

$$PM_{10} = 144.55 \times AOT + 33.031 (R^2 = 0.588). \quad (1)$$

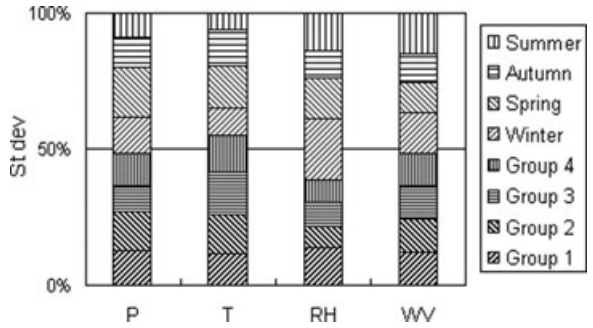

Fig. 3. The proportion of each season's and group's standard deviation of four meteorological parameters.

After grouping, the four meteorological variables in a group are homogenized while intragroup variation becomes more distinct than the season-based counterparts. The effectiveness of identifying the meteorological control over the closeness of the correlation is a comparative examination of the standard deviation of meteorological parameters. As illustrated in Fig. 3, all the four groups make up less than half of the total variation except temperature. The combined percentage is the lowest for relative humidity, but very close to the 50% threshold for pressure and wind velocity. The distribution of these percentages demonstrates once again that grouping of meteorological variables is better at identifying the conditions under which AOT is more equivalent of PM_{10}. This is explained by the fact that season, defined by temperature mostly, does not exhibit distinct variations across the border between two seasons. In fact, it could fluctuate widely on these border days. By comparison, clustering based on any of the meteorological parameters is able to produce much more homogenous membership in a group. This grouped manner of data analysis is more conducive to revealing the meteorological conditions under which PM_{10} is best monitored from AOT.

3.3. Capability of air pollution monitoring

As shown in Table 5, two seasons (spring and winter) have a low correlation coefficient at a combined number of 88 days or 56.05% of the total observations if analysed by season. In other words, air pollution in more than half of the 157 observations cannot be reliably monitored by means of remote sensing. This high percentage suggests that the days on which air quality can be monitored reliably by means of remote sensing are rather limited. By comparison, the number of observations that cannot be reliably estimated (e.g. having a large root mean squared error or RMSE) drops to only 26 (16.56% of the total) after being clustered. This means that grouping by meteorological similarity is superior to season-based analysis in reducing the number of observations that do not allow air pollution to be adequately sensed.

In addition, Table 5 shows that the most severely polluted season is spring ($PM_{10} = 130.04\ \mu gm^{-3}$) while summer has the lowest pollution level ($PM_{10} = 105.56\ \mu gm^{-3}$). The pollution level stays nearly the same in winter and autumn. The level of air pollution is rather high at $122.28\ \mu gm^{-3}$ for the winter season in 2004. This value is much larger than $101.62\ \mu gm^{-3}$ derived from the 26 observations. On the other hand, the summer pollution level is detected over $110\ \mu gm^{-3}$, higher than $105.56\ \mu gm^{-3}$ for the entire season. The monitored pollution level is actually lower than the reality in winter but higher in summer. Moreover, the monitoring accuracy level from the MODIS data is inversely related to the pollution level. The winter and spring seasons with a larger PM_{10} have a lower correlation coefficient and a large RMSE. Furthermore, the number of days on which remote sensing monitoring is feasible is also limited (e.g. 26 days in winter). This means that the accuracy of monitoring air pollution is low when the pollution level is relatively high on a limited number of days. This is not ideal as in reality it is the most serious pollution situation that should be accurately monitored.

4. Conclusions

The AOT information acquired from MODIS data can reflect the amount of suspended particulates in the atmosphere. This indicator of accumulative particles over the vertical column may bear a close correlation with ground observed PM_{10} in certain seasons, subject to meteorological conditions. In general, the correlation is weak for all observations under a diverse range

Table 5. Comparison of air pollution level by season and by clustering analysis

	Group 1	Winter	Group 2	Spring	Group 3	Autumn	Group 4	Summer
No. of obs.	26	26	49	62	51	45	31	24
(% of total)	(16.56)	(16.56)	(31.21)	(39.49)	(32.48)	(28.66)	(19.75)	(15.29)
% of season duration		28.89		68.89		50.00		26.67
PM_{10} (μgm^{-3}) from obs.	106.54	101.62	132.28	128.52	120.44	121.96	110.20	113.00
2004 PM_{10} (μgm^{-3})		122.28		130.04		125.62		105.56
Corr. coefficient	0.45	0.47	0.62	0.52	0.77	0.80	0.73	0.87
RMSE	30.77	26.22	24.69	28.26	24.17	21.80	26.06	22.45

of environmental conditions. Seasonally, the relationship is the closest in summer and autumn with a coefficient over 0.80, but weaker in spring and winter at around 0.50. Analysis of clustered data maintains a close correlation between PM_{10} and AOT for three of the four groups. Besides, the number of days on which air pollution cannot be reliably monitored is reduced from 88 to 26 after all observations are grouped by meteorological similarity. It is more reliable to monitor PM_{10} from MODIS AOT data at a high temperature and relative humidity, but a low pressure and wind velocity. There is an inverse relationship between the pollution level and the accuracy at which it is monitored from the MODIS data. These findings should serve as useful guidance in selecting the appropriate meteorological conditions under which air pollution can be monitored reliably from MODIS AOT data.

5. Acknowledgments

We thank the three anonymous reviewers for their helpful comments. The data used in this study were acquired as part of the NASA's Earth Science Enterprise. The algorithms were developed by the MODIS Science Teams. The data were processed by the MODIS Adaptive Processing System (MODAPS) and Goddard Distributed Active Archive Center (DAAC), and are archived and distributed by the Goddard DAAC. The PM and meteorological data were acquired from the Data Centre of the Chinese Ministry of Environmental Protection, and the China Meteorological Data Sharing Service System, respectively. This research was funded by the National Science and Technology Support Plan of China (No. 2008BAC34B07). Additional funding was received from the Key Fundamental Research Projects of Natural Science in Universities affiliated with the Jiangsu Province (No. 08KJA170001), and the Key Short-term Projects of Inviting Overseas Experts to Universities affiliated with the Jiangsu Province, China.

References

Chu, D. A., Kaufman, Y. J., Zibordi, G., Chern, J. D., Mao, J., and co-authors. 2003. Global monitoring of air pollution over land from the Earth Observing System-Terra Moderate Resolution Imaging Spectroradiometer (MODIS). *J. Geophys. Res.* **108**(D21), 4661, doi:10.1029/2002JD003179.

Engel-Cox, J. A., Hoff, R. M. and Haymet, A. D. J. 2004a. Recommendations on the use of satellite remote-sensing data for urban air quality. *J. Air Waste Manage. Assoc.* **54**, 1360–1371.

Engel-Cox, J. A., Holloman, C. H., Coutant, B. W. and Hoff, R. M. 2004b. Qualitative and quantitative evaluation of MODIS satellite sensor data for regional and urban scale air quality. *Atmos. Environ.* **38**, 2495–2509.

Gupta, P., Christopher, S. A., Wang, J., Gehrig, R., Lee, Y., and co-authors. 2006. Satellite remote sensing of particulate matter and air quality assessment over global cities. *Atmos. Environ.* **40**, 5880–5892.

Hutchison, K. D. 2003. Applications of MODIS satellite data and products for monitoring air quality in the state of Texas. *Atmos. Environ.* **37**, 2403–2412.

Hutchison, K. D., Smith, S. and Faruqui, S. 2004. The use of MODIS data and aerosol products for air quality prediction. *Atmos. Environ.* **38**, 5057–5070.

Hutchison, K. D., Smith, S. and Faruqui, S. J. 2005. Correlating MODIS aerosol optical thickness data with ground-based $PM_{2.5}$ observations across Texas for use in a real-time air quality prediction system. *Atmos. Environ.* **39**, 7190–7203.

Kaufman, Y. J., Tanr, D., Remer, L. A., Vermote, E. F., Chu, A., and co-authors. 1997a. Operational remote sensing of tropospheric aerosol over the land from EOS-MODIS. *J. Geophys. Res.* **102**(D14), 17051–17067.

Kaufman, Y. J., Wald, A. E., Remer, L. A., Gao, B.-C., Li, R.-R., and co-authors. 1997b. The MODIS 2.1μm channel—correlation with visible reflectance for use in remote sensing of aerosol. *IEEE Trans. Geosci. Remote Sens.* **35**, 1286–1298.

King, M. D., Kaufman, Y. J., Menzel, W. P. and Tanré, D. 1992. Remote sensing of cloud, aerosol, and water vapor properties from the Moderate Resolution Imaging Spectrometer (MODIS). *IEEE Trans. Geosci. Remote Sens.* **30**, 2–27.

Lee, J. and Kim, Y. 2007. Spectroscopic measurement of horizontal atmospheric extinction and its practical application. *Atmos. Environ.* **41**, 3546–3555.

Li, C. C., Lau, A. K. H., Mao, J. and Chen, A. 2004. An aerosol pollution episode in Hong Kong with remote sensing products of MODIS and LIDAR. *J. Appl. Meteorol. Sci.* **15**, 641–650.

Li, C. C., Mao, J. T., Lau, A. K. H., Liu, X. Y., Liu, G. Q., and co-authors. 2003a. Research on the air pollution in Beijing and its surroundings with MODIS AOD products. *Chin. J. Atmos. Sci.* **27**, 869–880.

Li, C. C., Mao, J. T. and Lau, A. K. H. 2003b. Characteristics of aerosol optical depth distributions over Sichuan basin derived from MODIS data. *J. Appl. Meteorol. Sci.* **14**, 1–7.

Liu, G. Q., Li, C. C., Zhu, A. H. and Mao, J. T. 2003. Optical depth research of atmospheric aerosol in the Yangtze River Delta region. *Environ. Prot.* 2003, 50–54.

Mao, J. T., Li, C. C., Zhang, J. H., Liu, X. Y. and Lau, A. K. H. 2002. The comparison of remote sensing aerosol optical depth from MODIS data and ground sun2photometer observations. *J. Appl. Meteorol. Sci.* **13**(Suppl), 127–135.

Suresh, T. and Desa, E. 2005. Seasonal variations of aerosol over Dona Paula, a coastal site on the west coast of India. *Atmos. Environ.* **39**, 3471–3480.

Wang, H. 2006. *Regression Analysis of Air Pollution Indices against MODIS Aerosol Optical Thickness in Nanjing*. Master's thesis of Nanjing Normal University, 55 p.

Wang, H. and Zha, Y. 2006. MODIS-derived aerosol optical thickness as an indicator of urban air quality. *Urban Environ. Urban Ecol.* **19**, 21–24.

Wang, J. and Christopher, S. A. 2003. Intercomparison between satellite-derived aerosol optical thickness and PM2.5 mass: implications for air quality studies. *Geophys. Res. Lett.* **30**(21), 2095, doi:10.1029/2003GLO18174.

Zakey, A. S., Abdelwahab, M. M. and Makar, P. A. 2004. Atmospheric turbidity over Egypt. *Atmos. Environ.* **38**, 1579–1591.